The Effect of Ions on the Optical Absorption Spectra of Aqueously Solvated Chromophores

Sapana V. Shedge,[1] Tim J. Zuehlsdorff,[1] Michael J. Servis,[2] Aurora E. Clark,[2,3] and Christine M. Isborn[1,a)]
[1)] *Chemistry and Chemical Biology, University of California Merced, Merced, California 95343, United States*
[2)] *Department of Chemistry and the Material Science and Engineering Program, Washington State University, Pullman, Washington 99164, United States*
[3)] *Pacific Northwest National Laboratory, Richland, WA, 99352 United States*

(Dated: 27 January 2020)

In the condensed phase, ions often create heterogeneous local environments around a solute, which may impart chemical reactivity or perturbations to physico-chemical properties. Although the former has been the subject of some study, the latter - particularly as is pertains to optical absorption spectroscopy - is much less understood. In this work, the computed UV-Vis absorption spectrum is examined for the aqueously solvated chromophore anion of green fluorescent protein for different local ion configurations. The strong ability of water to screen the ions from the chromophore results in little change in excitation energy compared to a purely aqueous environment. However, upon forming a contact ion pair with a sodium ion at either of the two electronegative oxygen sites of the chromophore, there is a spectral shift to either higher or lower energies. Surprisingly, our analysis suggests that the cause of the spectral shift is dominated not by the electrostatic presence of the ion, but instead by ion disruption of the hydrogen bond network at the oxygen contact ion pair site.

I. INTRODUCTION

The heterogeneous environment provided by ions in aqueous solution can drive chemical reactions,[1,2] govern the structure and function of biomolecules,[3–5] and influence photocatalytic reactivity and selectivity.[6–8] Often the solvated ions create an electrostatic potential or transfer of charge to drive the reaction, but they also affect the hydrogen bonding of the aqueous medium. A variety of studies suggest that ions lead to the perturbation to the electronic structure of bulk water due to a combination of the electrostatic presence of the ion and the distortion of the hydrogen bond network in the first solvation shell of the ion.[9–26]

Although the optical absorption of anionic chromophores is of interest in both biology and energy related applications, it is unclear how the non-absorbing ions in solution with the chromophore affect the optical absorption. Perturbations to the optical absorption may occur due to the continuum field caused by the background electrolyte or due to a local change to aqueous solvation about a chromophore caused by ion disruption of the hydrogen bond network of water. The concentration of ions may be substantial under solution conditions of high/low pH or high ionic strength. The optical properties of the green fluorescent protein (GFP) chromophore anion have been highly studied because it is thought that the GFP chromophore exists in its anionic state in its native protein environment.[27,28] In the case of the optical absorption spectrum of the GFP chromophore in aqueous solution, the chromophore is kept deprotonated at pH=13 in aqueous 1M NaOH,[29] creating a highly ionic environment for the anionic chromophore which may affect the optical absorption spectrum.

Simulating the effect of ions on optical absorption spectra presents a challenge. An explicit treatment of the electronic structure of large regions of solvent is known to be necessary for capturing solute-solvent polarization and charge-transfer interactions for chromophores in solution,[30–40] and it is therefore likely also necessary to treat ions at quantum mechanical (QM) level if ions are in the first solvation shell of the chromophore. Although many experiments are performed in multi-component solutions, spectral simulations of a chromophore are generally performed at the infinite dilution limit, ignoring all ions in the environment. For example, despite the highly ionic environment of the GFP chromophore anion at high pH, most calculations of the absorption spectrum of this system resort to continuum solvent models (e.g., refs.[41–43]) that only use the dielectric constant of water and do not account for any perturbation induced by ion solutes. Two of the authors have recently reported computed spectra for the GFP anionic chromophore,[44,45] wherein we explicitly accounted for the solvent environment by using an ensemble method[35,38,46–48] to include chromophore-solvent configurations from a molecular dynamics (MD) simulation in the computed spectrum. Our new method of including explicit solvent and also taking into account vibronic effects[44] led to much improved lineshapes over continuum approaches,[41–43] but our simulated spectrum[44,45] remained more narrow than the experimental spectrum. However, the ions neglected in the MD simulation may be the key to this missing spectral width.

In the present work, we examine how ions affect the simulated absorption spectrum of the aqueously solvated

[a)] Electronic mail: cisborn@ucmerced.edu

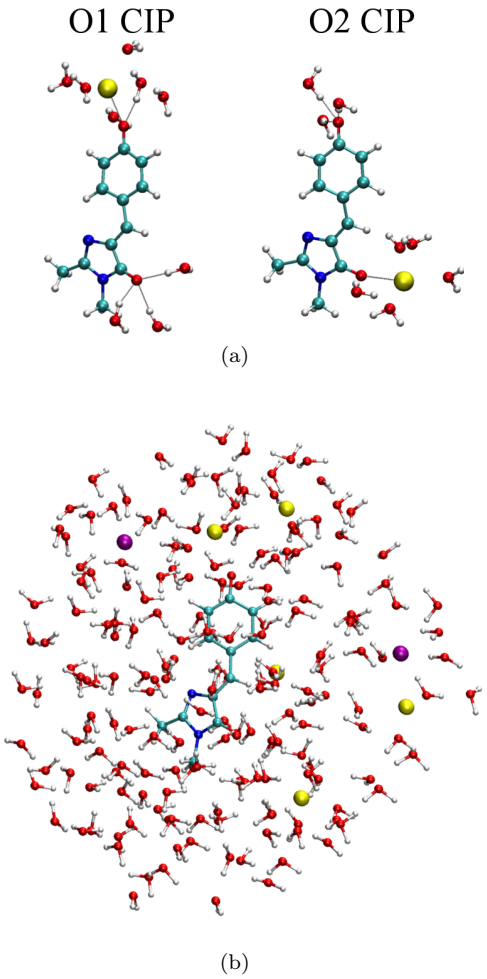

FIG. 1. (a) Structure of the green fluorescent protein (GFP) chromophore anion and Na^+ ion for the two contact ion pair configurations. The two electronegative oxygen sites analyzed in this work are illustrated with water solvating the oxygen sites and contact ion pairs for the phenolate O1 oxygen (left) and the imidazolinone O2 oxygen (right).Dashed lines indicate ion pairing and hydrogen bonding. Color coding of the atoms: cyan = carbon, red = oxygen (O1:Phenolate oxygen,O2:imidazolinone-4 oxygen), blue = nitrogen, white = hydrogen, yellow = sodium. (b) The QM region used for excited state calculations. The QM region is shown for an MD snapshot of the GFP chromophore anion in 1M aqueous NaCl. The QM region includes the chromophore anion and the nearest water molecules and ions (yellow = sodium, purple = chloride).

anionic chromophore of GFP. We use classical MD simulations to generate the instantaneous structure of the chromophore in ionic aqueous solution. We analyze the direct and the indirect effects of the ion on the computed excited energies and optical absorption spectrum. We find that the disruption of the hydrogen-bonding network by the formation of contact ion pairs (CIPs) at two sites on the chromophore (see Fig. 1a) is the dominant factor controlling excitation energy shifts and leading to spectral broadening.

II. METHODS

A. Molecular dynamics

Although experimental studies employ 1M NaOH to keep the chromophore deprotonated,[29] obtaining the correct solvation structure of hydroxide anion using non-polarizable force fields is notoriously challenging.[49] We therefore pursued our studies of the effect of ionic environment on optical absorption spectra using aqueous NaCl solution. The initial configuration for the molecular dynamics simulation was generated with Packmol[50], with the 1 GFP anion, 87 Na^+, 86 Cl^- and 4300 H_2O molecules distributed randomly in a cubic cell of side length 51.23 Å after volume equilibration. After the 1 ns of equilibration in the NPT ensemble using the Berendsen barostat[51] to maintain a pressure of 1 bar with a 2 ps coupling time and the Berendsen thermostat[51] to maintain a temperature of 300 K with a 0.4 ps coupling time, the simulation was ran in the NVT ensemble for 40 ns at 300 K using the Nosé-Hoover thermostat[52] with a 0.4 ps coupling time. Long-range electrostatics were calculated using PME, with a real space cutoff of 15 Å for short-range electrostatics and for van der Waals interactions. Hydrogen-containing bonds were constrained using the LINCS algorithm.[53] Snapshots were taken for analysis at 10 ps intervals. That NVT simulation trajectory was followed by additional 40 ns to obtain contact ion pairing and solvent separated ion pairing probabilities. Simulations were conducted using the GROMACS 5.1.4 software package.[54] Water was modeled with SPC/E.[55] The Na^+ and Cl^- ions were modeled with the AMBER-99 force field[56] for pairwise interactions whereas the OPLS[57] Lennard-Jones parameters were used for the Na^+–Na^+, Na^+–Cl^- and Cl^-–Cl^- pairwise interactions to prevent unphysical ion clustering in solution, as recommended in ref. 58. The GFP anion was modeled with GAFF[59] using modified parameters discussed in Ref. 44.

B. Hydrogen bonding and ion pairing definitions

Hydrogen bonding and ion pairing were calculated from MD simulation trajectories using the ChemNetworks software package.[60] Chromophore oxygen-water hydrogen bonds were defined as having an O1–H_W or O2–H_W distance of no more than 2.5 Å and an O1...H_W–O_W angle of no more than 45°. O1 and O2 are the chromophore oxygen sites, as shown in Fig. 1a, and H_W and O_W are the water hydrogen and oxygen atoms. Contact ion pairs (CIPs) and solvent separated ion pairs (SSIPs) were identified using oxygen-sodium distance cut-offs, determined from the Na^+–O RDFs. A CIP was defined as a distance of less than 3.0 Åand an SSIP was defined as a distance between 3.0 Å and 5.5 Å. Each chromophore oxygen site for a given snapshot was separately counted as a CIP configuration if there was at least one CIP present, as an SSIP configuration if there were no CIPs

and at least one SSIP, and as having no IPs if there were no CIPs or SSIPs present.

C. Excited state calculations and spectral details

Calculations of vertical excitation energies are performed by treating significant parts of the solvent environment surrounding the chromophore at the QM level, whereas all other solvent atoms present in the MM box are included in the calculations as classical fixed point charges. Our previous studies have demonstrated that including all solvent molecules with centers of mass within 8 Å of any atom of the chromophore in the QM region yields well-converged excitation energies in comparable systems.[31,36,38,39] However, due to the large number of ions present in the calculations, care has to be taken when defining the boundaries of the QM region in the electronic structure calculations. Using a simple 8 Å cutoff radius for both the solvent molecules and the ions yields a significant number of snapshots where QM ions are located at the boundary of the QM region, see example in the Supporting Information (SI). These snapshots, where the ions treated at the QM level are not properly screened by QM water molecules, generally show poor convergence within the self-consistent field calculations. To improve the treatment of the boundary of the QM region, we adjust our computational protocol for defining the QM region. First, all ions within 8 Å of any atom of the chromophore are included in the QM region. Water molecules are included in the QM region if their center of mass is either within 8 Å of any atom of the chromophore or 4 Å of any ion included in the QM region. This adjusted QM region significantly reduces the number of snapshots for which the electronic structure calculations fail to converge. The QM region for a representative snapshot is shown in Fig. 1b.

Vertical excitation energies for all snapshots are computed using linear-response TDDFT as implemented in the TeraChem code,[30,61–63] within the Tamm-Dancoff approximation.[64] All calculations are performed using the CAM-B3LYP functional[65] and a 6-31+G* basis set. Although a previous study[66] has shown that this basis set is too small to fully converge the absolute values of the excitation energies for the GFP chromophore, the present work examines changes in absorption spectra and spectral shape rather than the absolute position of absorption maxima. Absorption spectral shapes have been shown to be relatively robust with respect to changes in the basis set size.[44] For each snapshot, the two lowest singlet excitations are computed, with the lowest energy S_1 state always being the bright state of interest. This excited state is almost exclusively a HOMO→LUMO transition with charge transferring from the phenolate oxygen to the carbon backbone and imidazolinone ring (see SI for electron density difference).

The ensemble spectra are generated by taking each vertical excitation as a delta function, multiplied by the oscillator strength of that transition. Summing the delta functions of vertical excitations for every snapshot and convoluting them with a Gaussian function with a standard deviation of $\sigma = 21$ meV then yields the final ensemble spectra reported in this work. For easier comparison of spectra, all spectra are normalized to have an equal maximum intensity.

III. ANALYSIS OF ION/SOLUTE/SOLVENT CONFIGURATIONS AND THE RESULTING SPECTRAL SHIFTS

A. Molecular dynamics structural analysis

A potential of mean force for ion pairing at the O1 site was computed in the infinite dilution limit, as described and presented in the SI. Two minima in the Na^+–O1 distance reaction coordinate were identified: a contact ion pair (CIP) and solvent-separated ion pair (SSIP). From the concentrated NaCl molecular dynamics simulation, the CIP and SSIP probabilities of each oxygen site are reported with errors as the standard deviation of 20 ns block averages over the total 80 ns trajectory. For the O1 site, 3.1 ± 1.3% were observed to be CIP and 23.6 ± 2.4% SSIP with the remaining 73.3 ± 2.8% having no IP. For the O2 site, the same percents were 3.5 ± 1.7%, 18.9 ± 1.1% and 77.6 ± 2.1%, respectively. Within 58.4% ± 3.3% of snapshots no IP of either type (on either oxygen site) was observed. Within the equilibrium trajectory, the Na^+ position relative to the phenolate and imidazolinone rings and their effect on water solvation of the oxygen sites was analyzed and is reported in the SI.

The effect of contact and solvent separated ions pairs on water-chromophore hydrogen bonding at both chromophore oxygen sites was investigated for the concentrated NaCl molecular dynamics simulation, Table I. Subtle but consistent trends in the average chromophore oxygen-water hydrogen bond angle (O1...H_W–O_W and O2...H_W–O_W) and distance (O1–H_W and O2–H_W) were observed between snapshots with a CIP, SSIP, or no IP. The data indicates that CIPs slightly increase the O1–H_W and O2–H_W distances while slightly reducing the linearity of the O1...H_W–O_W and O2...H_W–O_W angles. The most significant change to the chromophore-water hydrogen bonding was the reduction in total number of hydrogen bonds in the presence of a CIP as a result of the Na^+ occupying the oxygen site, as shown in Tab. I. The data shows the differences and similarities in hydrogen bonding at the O1 and O2 sites: the average distance and angle of the hydrogen bonds at both oxygen sites are similar, but there is a significant reduction in the average number of hydrogen bonds independent of ion pairing such that the O1 site forms, on average, greater than 0.5 hydrogen bonds more at a time than the O2 site. Although there is a slightly larger negative charge on the O1 phenolate oxygen relative to the O2 imidazolinone oxygen, the adjacent methyl group at the O2 site

Hydrogen Bond	CIP		SSIP		No IP	
	O1	O2	O1	O2	O1	O2
Length [Å]	1.90	1.92	1.84	1.86	1.84	1.86
Angle [degrees]	158	155	161	159	161	160
Number	1.71	1.09	3.16	2.56	3.18	2.52

TABLE I. The average chormophore-water hydrogen bond distance (O1–H_W, O2–H_W), angle (O1...H_W–O_W,O2...H_W–O_W), and number are calculated for snapshots classified as a CIP, SSIP or no IP at each chormophore oxygen site.

reorganizes the local solvation environment and is likely the primary source for the decreased hydrogen bonding relative to the O1 site.

B. Screening of distant ions by water

Before examining the spectral changes induced by formation of either contact IPs or solvent-separated IPs, we first examine the ensemble spectrum obtained from the 1M NaCl solution configurations with no IPs. Comparing the spectrum obtained using these configurations to the spectrum obtained from the single Na^+ ion trajectory will allow us to assess the effects of distant ions on the spectrum. TDDFT excitation energies and oscillator strengths were computed for each snapshot using the QM region described in section II C. The resulting ensemble spectra are shown in the SI. The spectra for the two environments are similar in both energy, width, and spectral shape, suggesting that the concentrated ionic environment beyond the first solvation shell is effectively screened by a layer of QM water. Spectra computed with a fully MM environment (solvent and ions) using the same snapshots are also similar to each other (see SI), indicating that water molecules treated with fixed point charges also effectively screen the distant ion charges from polarizing the chromophore.

C. Spectral shifts from chromophore-ion interactions

We next compare absorption spectra obtained from snapshots of ion-pairs (CIPs and SSIPs) to determine how these chromophore-ion interactions alter the excitation energies. The computed ensemble spectra obtained using the CIP and SSIP configurations for the O1 site are shown in Fig. 2 (upper panel). We find that ion pairing at the O1 site results in a spectral red-shift compared to the no IP spectra. In contrast, the ensemble spectra obtained using the CIP configurations for the O2 site, Fig. 2 (lower panel), show a spectral blue-shift. These spectral shifts due to ion pairing have the potential to broaden the overall ensemble spectrum, leading to better agreement with the experimental spectrum compared to methods neglecting ions in the solvent environment.

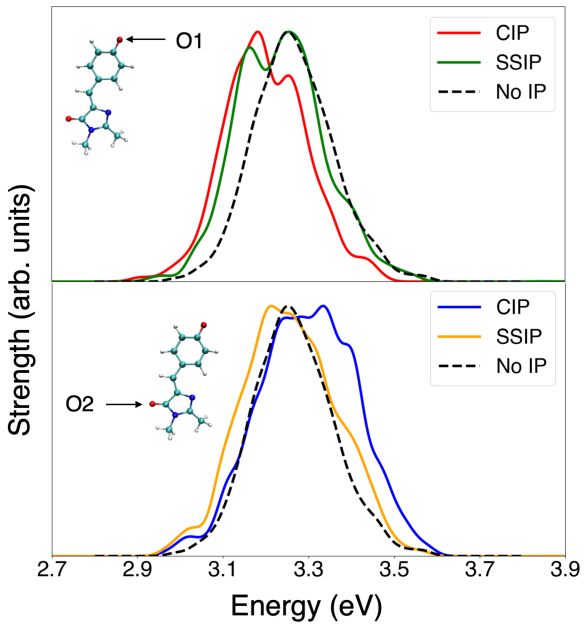

FIG. 2. Computed ensemble absorption spectra for the GFP chromophore anion in 1M aqueous NaCl using different subsets of configurations: contact ion pair of Na^+ with the chromophore at O1 (red, 380 snapshots), solvent separated ion pair at O1 (green, 424 snapshots), contact ion pair at O2 (blue, 466 snapshots), solvent separated ion pair at O2 (orange, 440 snapshots), and no ion pairing (black, 1015 snapshots).

Interestingly, we find that the spectral shift of these ion-pairing configurations is only captured by a QM treatment of the nearby environment. The comparison of absorption spectra simulated using QM/MM and MM solvent environment for CIP snapshots is shown in Fig. 3. The use of fixed point charges for the solvent and ions in the TDDFT calculations results in very similar ensemble spectra for the two sets of CIPs. This result not only highlights the importance of QM treatment of subset of solvent around the chromphore in order to get reliable position of absorption maxima and line shape, it also suggests that the charge transfer and mutual polarization captured with a QM treatment of the environment is key to capturing these ion-induced spectral shifts.

The close proximity of the Na^+ to the chromophore may lead to an altered chromophore geometry. Previous studies[45,67] have shown that the carbon-carbon and carbon-nitrogen bond of the chromophore backbone strongly couples to the optical excitation, so any systematic changes in the chromophore bond lengths due to the ion will likely lead to spectral shifts. To test this hypothesis, we removed the environment around the chromohore for the CIP snapshots at both oxygen sites and then recomputed the excitation energies for each chromophore configuration, now in vacuum. Using these new excitation energies, we recomputed the ensemble spectra. The

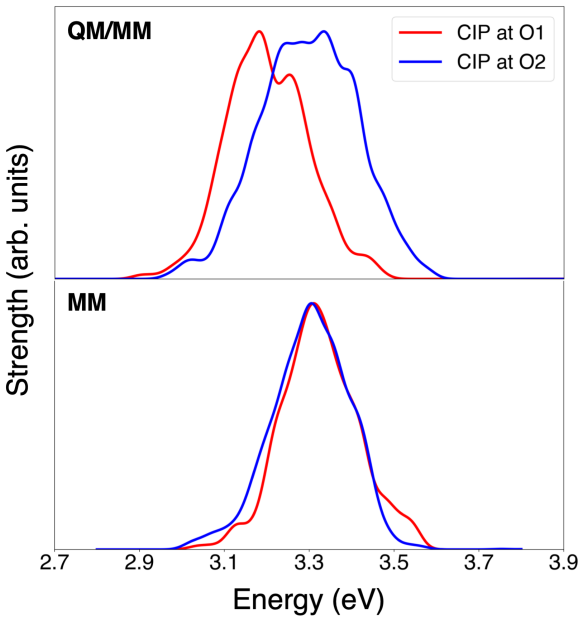

FIG. 3. Computed ensemble absorption spectra for GFP chromophore anion in 1M aqueous NaCl for contact ion pair configurations at O1 (red, 380 snapshots) and at O2 (blue, 466 snapshots). Results in the upper panel used a large QM region of solvent and ions around the chromophore whereas results in the lower panel used a fixed point MM charge model for the solvent and ion environment.

resulting computed ensemble spectra for configurations of the chromophore in vacuum are shown in the SI. The spectra computed with the chromophore configurations from the two different CIP oxygen sites are nearly identical. The similarity of the spectra indicates the geometries sampled by the chromophore are very similar for both CIP sites. This result is supported by chromophore bond length analysis shown in the SI. The dihedral angle measured between ion and two different oxygen sites of chromophore did not show any correlation with excitation energy as shown in the SI. These results suggest that the proximity of the Na^+ ion does not affect the chromophore geometry, thus changes in chromophore geometry are not responsible for the spectral shifts.

To better understand the origin of the spectral shifts seen upon ion-pair formation, in the next sections we analyze how the direct effects of the ion and the indirect effects of the ion changing the H-bonding environment correlate with changes in excitation energy.

1. Analysis of the Direct Effect of the Ion on the Chromophore Excitation Energy

We analyzed the direct effect of the ion on the chromophore's excitation energy by first examining how the proximity of the Na^+ ion within the CIP correlates with the excitation energy. A scatter plot of the computed excitation energy versus the distance of the ion from the oxygen site, shown in the SI for both sets of CIP configurations. There is a significant degree of noise in the data due to the heterogeneous distribution of the solvent environment along with the changes in the chromophore geometry during the MD. It is therefore difficult to determine any correlation between excitation energy and ion distance for this distribution of snapshots.

To isolate the effect of the ion from the heterogeneous environment and changes in chromophore geometry over each MD snapshot, we analyzed the excitation energy trends of a small subset of CIP snapshots in greater detail. For these snapshots, we varied the distance of the Na^+ ion from the oxygen site while keeping the remaining atoms fixed. The excitation energy was then recomputed for each chromophore-Na^+ distance. Fig. 4 (first column) shows how the excitation energy changes as the ion is moved closer to and further from the oxygen site for the large QM region used for the spectral calculations. For the CIP at the O1 site, the excitation energy increases as the Na^+ ion-O1 distance decreases, whereas for the CIP at the O2 site, the excitation energy decreases as the Na^+ ion - O2 distance decreases. We performed the same analysis with a fixed point charge MM treatment of the environment, see Fig. 4 (second column). For this MM model, we observe similar trends as with the QM environment. The similar result with the QM and MM treatments of the environment indicates that the change in excitation energy due to the presence of the ion is primarily an electrostatic, rather than a charge-transfer, interaction.

The shift in excitation energy suggests that the Na^+ ion at the O1 site stabilizes the ground state when more electron density is on the phenolate oxygen, whereas the Na^+ ion at the O2 site stabilizes the excited state when more electron density is on the imidazolinone oxygen (see SI for electron density difference for the ground and excited state). Surprisingly, for both oxygen CIP sites, the shift in excitation energy is in the *opposite* direction of the spectral shift computed in Fig. 2. Additionally, very little shift in the spectrum was seen for an MM environment in Fig.3, but the Na^+ distance scan does predict an energy shift with an MM environment, showing that the proximity of Na^+ alone is not the source of the spectral shift. These two discrepancies suggest that the electrostatic presence of the ion is not responsible for the spectral differences computed for the two CIP sites. Instead, it is likely the indirect effects of the presence of the ion, such as changes in H-bonding, that dominate the observed spectral changes. We analyze these effects in the next section.

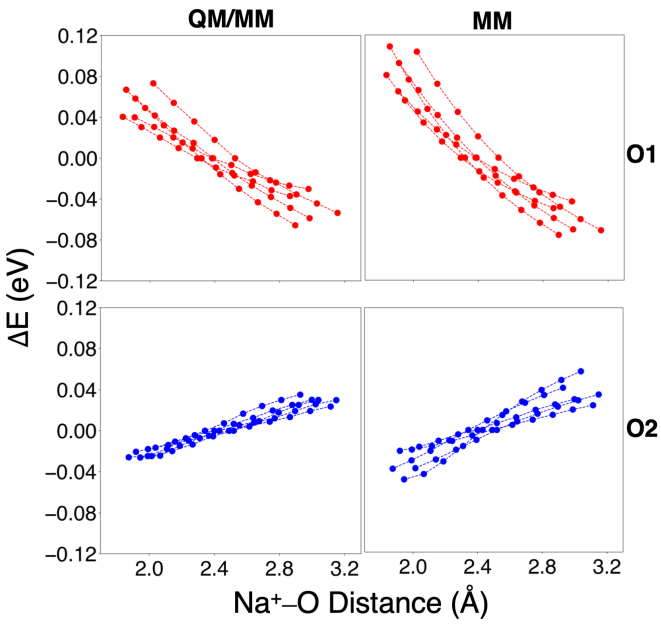

FIG. 4. The change in excitation energy (eV) versus the Na^+-O distance (Å). The upper panel shows the change in excitation energy versus Na^+-O1 distance (Å) in the QM/MM environment (on left) and in the purely MM environment (on right). The lower panel shows the change in excitation energy versus Na^+-O2 distance (Å) in the QM/MM environment (on left) and in the purely MM environment (on right). The QM/MM environment has the large QM region shown in Fig.1b and the MM environment treats all solvent molecules and ions surrounding the chromophore as fixed point charges in the TDDFT calculation. The 0.00 value of ΔE is the value computed for the unaltered snapshot.

2. Analysis of the Indirect Effects of the Ion on the Chromohore Excitation Energy: Changes in hydrogen bonding

To determine why the computed ensemble spectrum for ion pairs shifts in the opposite direction for what would be expected based on the excitation energies analyzed in the previous section, we next analyze the indirect changes in the solvent environment caused by ion pair formation. The hydrogen bond analysis shown in Table I indicates that ion pair formation disrupts the hydrogen bonding network around the O1 and O2 sites. On average, the Na^+ ion replaces 1.5 hydrogen bonds at both oxygen sites of the chromophore. Additionally, of the remaining H-bonds, the average hydrogen bond length is increased compared to configurations with no ion pairing. Thus the hydrogen bond environment around the oxygens is weakened upon CIP formation for both sites.

Following a similar analysis as we performed for Na^+, we looked for correlation of hydrogen bond strength with excitation energy. In the SI we show the computed excitation energy versus the bond length of the shortest of the hydrogen bonds formed between water and the oxygen site of the CIP. There is again a considerable degree of scatter in the excitation energies, as would be expected for a heterogeneous environment. We therefore analyzed a subset of snapshots where we changed the H_w...O1 and H_w...O2 length by moving only the hydrogen atom of the water while keeping all other atoms fixed. Fig. 5 shows that when treating the environment with QM, as the H_w...O1 and H_w...O2 distance decreases, the excitation energies increases for the O1 site and decreases for the O2 site. This trend is similar to the trend seen in Fig. 4 where we varied the Na^+-chromophore distance. Although an MM treatment of the environment provided a similar trend as the QM environment for the Na^+ scan in Fig. 4, this is not the case for the H-bond scan in Fig. 5. With an MM fixed point charge environment, there is a much smaller shift in energy for the O1 site whereas the shift in excitation energy is negligible at the O2 site. This lack of shift with the point charge environment suggests that the energy shift due to the change in H-bond strength may require charge transfer between the chromophore and the H-bonding solvent. The different shifts in excitation energy for the QM versus MM environment are consistent with Fig. 3, supporting that changes in H-bonding are likely responsible for spectral differences for the two CIP sites.

To isolate the effects of the altered solvent environment from the electrostatic presence of the Na^+ ion, we recomputed the ensemble absorption spectrum from the CIP snapshots, but removed the Na^+ ion involved in CIP formation. If the ion was directly responsible for the spectral shift, we would expect that deleting the ion would shift the CIP spectra closer to those with no ion pairing in Fig. 2, where the more distant ions are screened by the solvent. However, Fig. 6 shows that, upon deletion of the CIP Na^+ ion, the spectrum instead shifts to lower energies for the configurations from the O1 CIP and to higher energies for the O2 CIP. By removing the Na^+ ion, the shift caused by the changes in the solvent environment due to the presence of the ion are emphasized: *the change in the H-bonding environment is responsible for the spectral shifts of the CIP configurations.*

IV. SIMULATED SOLUTION PHASE SPECTRA AND COMPARISON WITH EXPERIMENT

In this section we compare our results to the experimental absorption spectrum of the GFP chromophore in aqueous solution. The ensemble method[30,35,38,46–48,68] we have used thus far captures the effects of explicit chomophore-environment interactions. However, for comparison of our simulated spectra to experiment, we have found that it is important also to add the effects of vibronic transitions. The vibronic spectrum can be computed within the Franck-Condon approach, but recent Franck-Condon simulations of the GFP chromophore using implicit solvent and Gaussian broadening to account for inhomogeneous solvent effects produced a spectrum

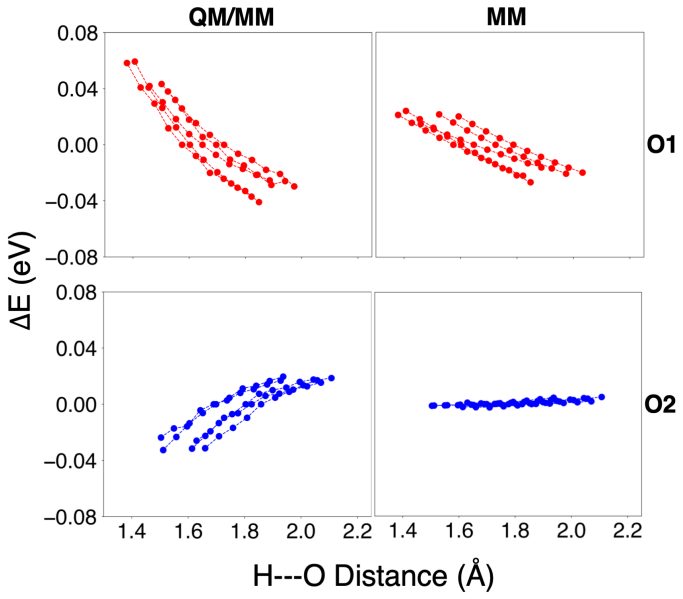

FIG. 5. The change in excitation energy (eV) versus the hydrogen bond H—O distance (Å). The upper panel shows the change in excitation energy versus H—O1 distance (Å) in the QM/MM environment (on left) and in the purely MM environment (on right). The lower panel shows the change in excitation energy versus H—O2 distance (Å) in the QM/MM environment (on left) and in the purely MM environment (on right). The QM/MM environment has the large QM region shown in Fig. 1b and the MM environment treats all solvent molecules and ions surrounding the chromophore as fixed point charges in the TDDFT calculation. The 0.00 value of ΔE is the value computed for the unaltered snapshot.

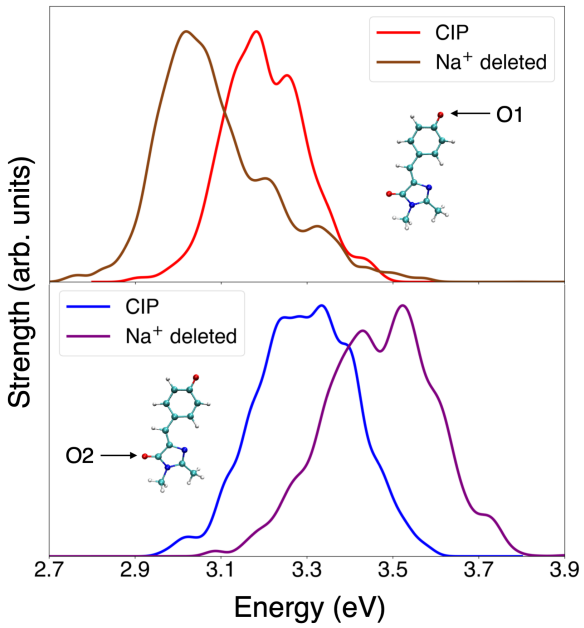

FIG. 6. Computed ensemble spectra for GFP chromophore anion CIP configurations with full environment and with the Na^+ ion deleted from the CIP. Red and blue are reference spectra from Fig. 2 for the CIP at the O1 site (380 snapshots) and for the CIP at the O2 (466 snapshots), respectively. Using the same snapshots with the Na^+ ion deleted from the CIP, the corresponding spectra are shown in brown and purple.

that was too narrow.[41–43] Specifically, a broadening parameter that was up to three times larger than that which would be predicted based on the solvent reorganization energy was necessary to generate a spectrum that was of comparable width to the experimental spectrum.[42] Here we will apply a new method developed by two of the authors that combines the ensemble method with a zero-temperature Franck-Condon shape function.[44,45,68] This E-ZTFC approach treats all temperature effects classically through the MD ensemble sampling and all vibronic transitions of the chromophore at zero temperature (vibronic transitions originate only from the ground state vibrational levels). Although the E-ZTFC method possesses some double counting of the nuclear degrees of freedom of the chromophore[44], the agreement with experimental spectra is good for the systems studied thus far and the method is a promising approach for capturing both vibronic effects and specific solute-environment effects.

In the previous study of the absorption spectrum of the same chromophore by Zuehlsdorff et al.,[45] AIMD and AI-PIMD simulations of the chromophore in a small, periodic water box were performed to obtain the ensemble of chromophore-solvent configurations for use in the E-ZTFC simulation of the spectrum. We found that the inclusion of nuclear quantum effects (NQEs) through the PIMD led to a better agreement with the experimental spectrum compared to AIMD. Our analysis showed that the NQEs led to a broader distribution of H-bond strengths (both weaker and stronger), a softening of the heavy atom bonds in the chromophore that couple to the optically bright state, and a widening of the distribution of vertical excitation energies from more diverse solvation environments, overall leading to the computation of a broader absorption spectrum. However, despite the double counting of nuclear degrees of freedom of the chromophore, which should lead to an overly broad spectrum, the simulated spectrum was too narrow compared to the experimental spectrum.[29,45]

One key element was missing from these simulations: the ionic environment. Because of the high computational cost of AIMD and AI-PIMD simulations, it was not feasible to perform the simulations with a large enough solvent box to accommodate the diffusion of the ions with a DFT treatment of the environment. The missing ions may be responsible for the remaining spectral width. In the experiment,[29] the environment surrounding the chromophore was a 1M NaOH aqueous solution. Here we use a 1M NaCl aqueous solution with classical MD; we've shown in this work that the ionic environment is highly

screened by the water solvent and we only see spectral shifts due to the specific interactions of ion-pairing. To visualize the effects of these spectral shifts with the inclusion of vibronic effects, we use the same vibronic shape function as in Ref. 45 to generate the E-ZTFC spectrum using ensemble snapshots from the 1M NaCl trajectory.

In Fig. 7 is shown the experimental spectrum along with vibronically broadened spectra computed within the E-ZTFC approach using three different sets of ensemble snapshots with all spectra aligned energetically to have the same absorption maximum. From the 1 M NaCl classical MD trajectory in this work, we compare the absorption spectrum computed from ensemble snapshots with no ion pairing to that from 50% weight from CIPs at the O1 site and 50% weight from CIPs at the O2 site. The spectrum for the CIP only snapshots provides the most extreme example of ion-induced broadening. This CIP only spectrum shows some extra broadening compared to the no ion pairing spectrum, but the spectrum is still too narrow compared to the experiment. We also show the spectrum computed by Zuehlsdorff et al. in Ref. 45, where the ensemble snapshots are from an AI-PIMD trajectory of the chromophore in water with no ions in the environment. This spectrum is broader than either of those generated from the 1M NaCl classical trajectory.

In Ref. 45, we found that the NQEs included in the AI-PIMD simulation led to both stronger and weaker hydrogen bonds compared to the AIMD trajectory. This distribution of H-bonds would likely be even larger in the presence of CIPs, which would presumably increase the spectral shift. Although the broader spectrum obtained from the aqueous AI-PIMD trajectory compared to the 1M NaCl classical trajectory might suggest that the NQEs are a more significant factor than that of the ionic environment in determining the spectral shape, it is difficult to determine the validity of this comparison given the different potentials (FF MD versus DFT-based AI-PIMD). It may be that the effects of ions are larger given an ab-initio potential that could accommodate proton transfer and it may be that the NQEs could be important for ion pairing configurations. However, performing AI-PIMD simulations of a chromophore in a large enough solvent box to accommodate ion diffusion at the correct ionic concentration is a formidable computational task.

V. CONCLUSION

In this work, we study how ions in solution affect the excitation energy and optical absorption spectrum of the aqueously solvated chromophore of GFP. In particular, we investigate if the presence of ions, generally neglected in spectral simulations, is responsible for the spectral width missing in previous studies.[44,45] We find that in our simulations of the GFP chromophore aqueously solvated in 1M NaCl, rather than providing simple electrostatic noise in the solvent environment leading to spectral broadening, the ions only appear to shift the excitation

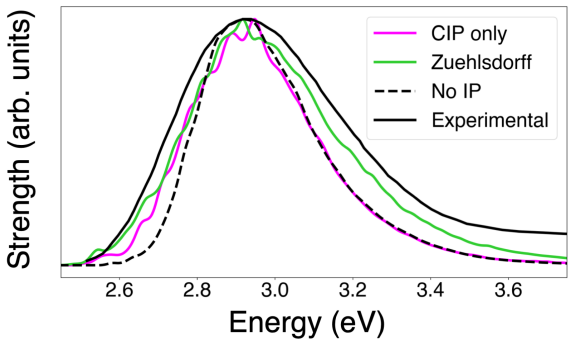

FIG. 7. Comparison of simulated ensemble absorption spectra with experimental spectrum. CIP only spectrum (magenta) includes the two sets of CIP configurations. No IP spectrum (black dotted line) includes snapshots with no ion-pairing around the chromophore. Zuehlsdorff spectrum (green) is computed using snapshots from AI-PIMD trajectories.[45] Experimental spectrum (black solid line)[29]. All computed spectra are shifted to align energetically and scaled to the same maximum height.

energies of the chromophore upon ion-pair formation. For both a QM and an MM treatment of the environment, the computed ensemble spectrum from snapshots of 1M NaCl with ions beyond the first solvation shell (no ion pairing) is nearly identical to that for a very dilute solution (only one Na^+ ion). The very effective screening of ions beyond the first solvation shell may be unique to water with its high dielectric constant.

Our MD analysis of the 1M NaCl trajectory shows contact ion pair formation at the two electronegative oxygen sites on the chromophore. CIP configurations for the phenolate O1 site produce a red-shift and CIP configurations for the imidazolinone O2 site produce a blue-shift. We find that it is necessary to treat the environment quantum mechanically to capture this spectral shift.

The dominant effect that ions have on the spectrum is through the disruption of the hydrogen bonding network, which only occurs if the ions are in the first solvation shell. Both the presence of the ion in the CIP and the H-bonds between the water and the chromophore at the O1 site stabilize the negative charge and the ground state, leading to higher excitation energy compared to the chromophore in a vacuum. However, the H-bonds between the water and the O1 site provide stronger stabilization than the Na^+ CIP, likely through improved charge transfer. Because the CIP disrupts the H-bonding network, the net result of CIP formation at the O1 site is less stabilization of the ground state and therefore a shift to lower excitation energies. Similarly, both the ion and H-bonding at the O2 site stabilize the excited state, but the H-bonds provide more stabilization than the ion; the net result of CIP formation at the O2 site is less stabilization of the excited state and therefore a shift to higher excitation energies.

For the chromophore environment of 1 M NaCl, the

simulations performed in this work show that the spectral broadening from ions is very small due to the small percentage of CIP configurations obtained in the trajectory. However, this small percentage may change with the use of an improved potential that accounts for mutual polarization or charge transfer or with the use of 1M NaOH instead of 1M NaCl. Additionally, ions may drive proton transfer or change the nature of the H-bonding beyond what can be modeled with a classical force field. Our two key findings that will hold in any aqueous environment are that (1) capturing specific chromophore-environment configurations and allowing for charge transfer between the chromophore and the local solvent structure is essential for simulating the full spectral shape and width and (2) the indirect changes in the local solvation environment caused by ion pairing may be larger than the direct electrostatic effects of the ion.

With continued advances in electronic structure and molecular dynamics methods and software, along with computing hardware, performing AI-PIMD simulations of chromophores in experimentally relevant ion concentrations may be feasible in the near future. This computational feat is likely necessary to provide the additional spectral width needed for the simulation to finally match experiment.

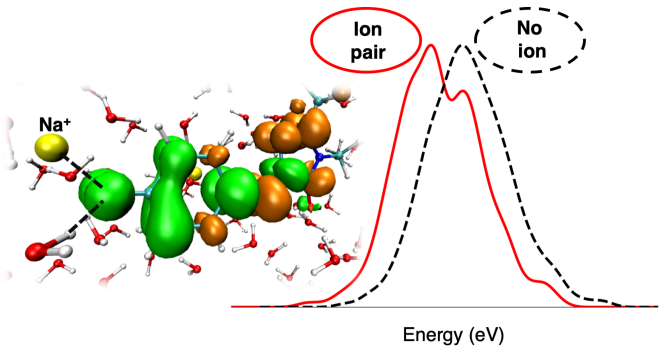

ACKNOWLEDGMENTS

This work was supported by the Department of Energy, Office of Basic Energy Sciences CTC and CPIMS programs, under Award Number DE-SC0014437. This work used the XStream and MERCED computational resources supported by the NSF MRI Program (Grants ACI-1429830 and ACI-1429783).

[1] M. S. Hegde, G. Madras, and K. C. Patil, "Noble metal ionic catalysts," Acc. Chem. Res. **42**, 704–712 (2009).
[2] C. Avanti, H. P. Permentier, A. van Dam, R. Poole, W. Jiskoot, H. W. Frijlink, and W. L. J. Hinrichs, "A new strategy to stabilize oxytocin in aqueous solutions: Ii. suppression of cysteine-mediated intermolecular reactions by a combination of divalent metal ions and citrate," Mol. Pharmaceutics **9**, 554–562 (2012).
[3] R. Hanna and J. A. Doudna, "Metal ions in ribozyme folding and catalysis," Curr. Opin. Chem. Biol. **4**, 166 – 170 (2000).
[4] S. A. Woodson, "Metal ions and rna folding: a highly charged topic with a dynamic future," Curr. Opin. Chem. Biol. **9**, 104 – 109 (2005).
[5] W. Maret and A. Wedd, eds., *Binding, Transport and Storage of Metal Ions in Biological Cells*, Metallobiology (The Royal Society of Chemistry, 2014) pp. P001–911.
[6] S. Higashimoto, R. Shirai, Y. Osano, M. Azuma, H. Ohue, Y. Sakata, and H. Kobayashi, "Influence of metal ions on the photocatalytic activity: Selective oxidation of benzyl alcohol on iron (iii) ion-modified tio2 using visible light," J. Catal. **311**, 137 – 143 (2014).
[7] Z. Li, L. Zhu, W. Wu, S. Wang, and L. Qiang, "Highly efficient photocatalysis toward tetracycline under simulated solar-light by $Ag^{+}-CDs-Bi_2WO_6$: Synergistic effects of silver ions and carbon dots," Appl. Catal. B-Environ **192**, 277–285 (2016).
[8] J. Kou, C. Lu, J. Wang, Y. Chen, Z. Xu, and R. S. Varma, "Selectivity enhancement in heterogeneous photocatalytic transformations," Chem. Rev. **117**, 1445–1514 (2017).
[9] H. Ohtaki and T. Radnai, "Structure and dynamics of hydrated ions," Chem. Rev. **93**, 1157–1204 (1993).
[10] A. W. Omta, M. F. Kropman, S. Woutersen, and H. J. Bakker, "Negligible effect of ions on the hydrogen-bond structure in liquid water," Science **301**, 347–349 (2003).
[11] C. D. Cappa, J. D. Smith, K. R. Wilson, B. M. Messer, M. K. Gilles, R. C. Cohen, and R. J. Saykally, "Effects of alkali metal halide salts on the hydrogen bond network of liquid water," J. Phys. Chem. B **109**, 7046–7052 (2005).
[12] L.-Å. Näslund, D. C. Edwards, P. Wernet, U. Bergmann, H. Ogasawara, L. G. M. Pettersson, S. Myneni, and A. Nilsson, "X-ray absorption spectroscopy study of the hydrogen bond network in the bulk water of aqueous solutions," J. Phys. Chem. A **109**, 5995–6002 (2005).
[13] C. D. Cappa, J. D. Smith, B. M. Messer, R. C. Cohen, and R. J. Saykally, "Effects of cations on the hydrogen bond network of

liquid water: new results from x-ray absorption spectroscopy of liquid microjets," J. Phys. Chem. B **110**, 5301–5309 (2006).
[14]A. K. Soper and K. Weckström, "Ion solvation and water structure in potassium halide aqueous solutions," Biophys. Chem. **124**, 180 191 (2006).
[15]S. Bouazizi, S. Nasr, N. Jadane, and M.-C. Bellissent-Funel, "Local order in aqueous nacl solutions and pure water: x-ray scattering and molecular dynamics simulations study," J. Phys. Chem. B **110**, 23515–23523 (2006).
[16]Y. Marcus and G. Hefter, "Ion pairing," Chem. Rev. **106**, 4585–4621 (2006).
[17]S. Park and M. D. Fayer, "Hydrogen bond dynamics in aqueous NaBr solutions," Proc. Natl. Acad. Sci. U.S.A. **104**, 16731–16738 (2007).
[18]J. D. Smith, R. J. Saykally, and P. L. Geissler, "The effects of dissolved halide anions on hydrogen bonding in liquid water," J. Am. Chem. Soc. **129**, 13847–13856 (2007).
[19]D. A. Turton, J. Hunger, G. Hefter, R. Buchner, and K. Wynne, "Glasslike behavior in aqueous electrolyte solutions," J. Chem. Phys. **128**, 161102 (2008).
[20]D. A. Schmidt, . Birer, S. Funkner, B. P. Born, R. Gnanasekaran, G. W. Schwaab, D. M. Leitner, and M. Havenith, "Rattling in the cage: Ions as probes of sub-picosecond water network dynamics," J. Am. Chem. Soc. **131**, 18512–18517 (2009).
[21]K. J. Tielrooij, N. Garcia-Araez, M. Bonn, and H. J. Bakker, "Cooperativity in ion hydration," Science **328**, 1006–1009 (2010).
[22]S. Funkner, G. Niehues, D. A. Schmidt, M. Heyden, G. Schwaab, K. M. Callahan, D. J. Tobias, and M. Havenith, "Watching the low-frequency motions in aqueous salt solutions: The terahertz vibrational signatures of hydrated ions," J. Am. Chem. Soc. **134**, 1030–1035 (2012).
[23]G. Stirnemann, E. Wernersson, P. Jungwirth, and D. Laage, "Mechanisms of acceleration and retardation of water dynamics by ions," J. Am. Chem. Soc. **135**, 11824–11831 (2013).
[24]I. Waluyo, D. Nordlund, U. Bergmann, D. Schlesinger, L. G. M. Pettersson, and A. Nilsson, "A different view of structure-making and structure-breaking in alkali halide aqueous solutions through x-ray absorption spectroscopy," J. Chem. Phys. **140**, 244506 (2014).
[25]P. Bajaj, X.-G. Wang, T. Carrington, and F. Paesani, "Vibrational spectra of halide-water dimers: Insights on ion hydration from full-dimensional quantum calculations on many-body potential energy surfaces," J. Chem. Phys. **148**, 102321 (2018).
[26]M. Riera, S. E. Brown, and F. Paesani, "Isomeric equilibria, nuclear quantum effects, and vibrational spectra of $M^+(H_2O)n{=}1{-}3$ clusters, with M = Li, Na, K, Rb and Cs, through many-body representations," J. Chem. Phys. A **122**, 5811–5821 (2018).
[27]L. M. Oltrogge and S. G. Boxer, "Short hydrogen bonds and proton delocalization in green fluorescent protein (GFP)," ACS Cent. Sci. **1**, 148–156 (2015).
[28]M. Chattoraj, B. A. King, G. U. Bublitz, and S. G. Boxer, "Ultra-fast excited state dynamics in green fluorescent protein: multiple states and proton transfer," Proc. Natl. Acad. Sci. U.S.A **93**, 8362–8367 (1996).
[29]S. B. Nielsen, A. Lapierre, J. U. Andersen, U. V. Pedersen, S. Tomita, and L. H. Andersen, "Absorption spectrum of the green fluorescent protein chromophore anion in vacuo," Phys. Rev. Lett. **87**, 228102 (2001).
[30]C. M. Isborn, A. W. Götz, M. A. Clark, R. C. Walker, and T. J. Martínez, "Electronic absorption spectra from mm and ab initio qm/mm molecular dynamics: Environmental effects on the absorption spectrum of photoactive yellow protein," J. Chem. Theory Comput. **8**, 5092–5106 (2012).
[31]C. M. Isborn, B. D. Mar, B. F. E. Curchod, I. Tavernelli, and T. J. Martínez, "The charge transfer problem in density functional theory calculations of aqueously solvated molecules," J. Phys. Chem.B **117**, 12189–12201 (2013).
[32]D. J. Cole, A. W. Chin, N. D. M. Hine, P. D. Haynes, and M. C. Payne, "Toward ab initio optical spectroscopy of the fenna-matthews-olson complex," J. Phys. Chem. Lett. **4**, 4206–4212 (2013).
[33]M. Retegan, F. Neese, and D. A. Pantazis, "Convergence of qm/mm and cluster models for the spectroscopic properties of the oxygen-evolving complex in photosystem ii," J. Chem. Theory Comput. **9**, 3832–3842 (2013).
[34]O. Valsson, P. Campomanes, I. Tavernelli, U. Rothlisberger, and C. Filippi, "Rhodopsin absorption from first principles: Bypassing common pitfalls," J. Chem. Theory Comput. **9**, 2441–2454 (2013).
[35]X. Ge, I. Timrov, S. Binnie, A. Biancardi, A. Calzolari, and S. Baroni, "Accurate and inexpensive prediction of the color optical properties of anthocyanins in solution," J. Phys. Chem. A **119**, 3816–3822 (2015).
[36]T. J. Zuehlsdorff, P. D. Haynes, F. Hanke, M. C. Payne, and N. D. M. Hine, "Solvent effects on electronic excitations of an organic chromophore," J. Chem. Theory Comput. **12**, 1853–1861 (2016).
[37]M. R. Provorse, T. Peev, C. Xiong, and C. M. Isborn, "Convergence of excitation energies in mixed quantum and classical solvent: Comparison of continuum and point charge models," J. Phys. Chem. B **120**, 12148–12159 (2016).
[38]T. J. Zuehlsdorff, P. D. Haynes, M. C. Payne, and N. D. M. Hine, "Predicting solvatochromic shifts and colours of a solvated organic dye: The example of nile red," J. Chem. Phys. **146**, 124504 (2017).
[39]J. M. Milanese, M. R. Provorse, E. Alameda, and C. M. Isborn, "Convergence of computed aqueous absorption spectra with explicit quantum mechanical solvent," J. Chem. Theory Comput. **13**, 2159–2171 (2017).
[40]M. Karelina and H. J. Kulik, "Systematic quantum mechanical region determination in qm/mm simulation," J. Chem. Theory Comput. **13**, 563–576 (2017).
[41]T. Huang, L. Yang, C. Zhu, and S. H. Lin, "Absorption and fluorescence spectra of the neutral and anionic green fluorescent protein chromophore: Franck-condon simulation," Chem. Phys. Lett. **541**, 110 – 116 (2012).
[42]F. J. Avila Ferrer, M. D. Davari, D. Morozov, G. Groenhof, and F. Santoro, "The lineshape of the electronic spectrum of the green fluorescent protein chromophore, part ii: Solution phase," ChemPhysChem **15**, 3246–3257 (2014).
[43]F. Zutterman, V. Liégeois, and B. Champagne, "Simulation of the uv/visible absorption spectra of fluorescent protein chromophore models," ChemPhotoChem **1**, 281–296 (2017).
[44]T. J. Zuehlsdorff and C. M. Isborn, "Combining the ensemble and franck-condon approaches for calculating spectral shapes of molecules in solution," J. Chem. Phys. **148**, 024110 (2018).
[45]T. J. Zuehlsdorff, J. A. Napoli, J. M. Milanese, T. E. Markland, and C. M. Isborn, "Unraveling electronic absorption spectra using nuclear quantum effects: Photoactive yellow protein and green fluorescent protein chromophores in water," J. Chem. Phys. **149**, 024107 (2018).
[46]J. P. Bergsma, P. H. Berens, K. R. Wilson, D. R. Fredkin, and E. J. Heller, "Electronic spectra from molecular dynamics: a simple approach," J. Phys. Chem. **88**, 612–619 (1984).
[47]R. Crespo-Otero and M. Barbatti, "Spectrum simulation and decomposition with nuclear ensemble: formal derivation and application to benzene, furan and 2-phenylfuran," Theor. Chem. Acc. **131**, 1237 (2012).
[48]A. V. Marenich, C. J. Cramer, and D. G. Truhlar, "Electronic absorption spectra and solvatochromic shifts by the vertical excitation model: Solvated clusters and molecular dynamics sampling," J. Phys. Chem. B **119**, 958–967 (2015).
[49]D. Marx, A. Chandra, and M. E. Tuckerman, "Aqueous basic solutions: Hydroxide solvation, structural diffusion, and comparison to the hydrated proton," Chem. Rev. **110**, 2174–2216 (2010).
[50]L. Martínez, R. Andrade, E. Birgin, and T. J. Martínez, "Packmol: A package for building initial configurations for molecular dynamics simulations," J. Comput. Chem. **30**, 2157–2164 (2009).

[51]H. Berendsen, J. Postma, W. van Gunsteren, A. DiNola, and J. Haak, "Molecular dynamics with coupling to an external bath," J. Chem. Phys. **81**, 3684 (1984).
[52]W. Hoover, "Canonical dynamics: Equilibrium phase-space distributions," Phys. Rev A **31**, 1695–1697 (1985).
[53]B. Hess, H. Bekker, H. Berendsen, and J. Fraaije, "Lincs: A constrained solver for molecular simulations," J. Comput. Chem. **18**, 1463–1472 (1997).
[54]M. Abraham, T. Murtol, R. Schulz, S. Pall, J. Smith, B. Hess, and E. Lindhal, "Gromacs: High performance molecular simulations through multi-level parallelism from laptops to supercomputers," SoftwareX **1-2**, 19–25 (2015).
[55]H. Berendsen, J. Grigera, and T. Straatsma, "The missing term in effective pair potentials," J. Phys. Chem. **91**, 6269–6271 (1987).
[56]J. Ponder and D. Case, "Force fields for protein simulations," Adv. Prot. Chem. **66**, 27–85 (2003).
[57]W. Damm, A. Frontera, J. Tirado-Rives, and W. Jorgensen, "OPLS all-atom force field for carbohydrates," J. Comput. Chem. **18**, 1955–1970 (1998).
[58]A. Chen and R. Pappu, "Parameters of monovalent ions in the amber-99 forcefield: Assessment of inaccuracies and proposed improvements," J. Phys. Chem. B **111**, 11884–11887 (2007).
[59]J. Wang, M. Romain, J. Caldwell, P. Kollman, and D. Case, "Development and testing of a general amber force field," J. Comput. Chem. **25**, 1157–1174 (2004).
[60]A. Ozkanlar and A. Clark, "ChemNetworks: a complex network analysis tool for chemical systems," J. Comp. Chem. **35**, 495–505 (2014).
[61]I. S. Ufimtsev and T. J. Martínez, "Quantum chemistry on graphical processing units. 3. analytical energy gradients and first principles molecular dynamics," J. Chem. Theory Comput. **5**, 2619–2628 (2009).
[62]C. M. Isborn, N. Luehr, I. S. Ufimtsev, and T. J. Martínez, "Excited-state electronic structure with configuration interaction singles and tamm-dancoff time-dependent density functional theory on graphical processing units," J. Chem. Theory Comput. **7**, 1814–1823 (2011).
[63]A. V. Titov, I. S. Ufimtsev, N. Luehr, and T. J. Martínez, "Generating efficient quantum chemistry codes for novel architectures," J. Chem. Theory Comput. **9**, 2213–221 (2013).
[64]S. Hirata and M. Head-Gordon, "Time-dependent density functional theory within the TammDancoff approximation," Chem. Phys. Lett. **314**, 291–299 (1999).
[65]T. Yanai, D. P. Tew, and N. C. Handy, "A new hybrid exchange-correlation functional using the Coulomb-attenuating method (CAM-B3LYP)," Chem. Phys. Lett. **393**, 51–57 (2004).
[66]E. Epifanovsky, I. Polyakov, B. Grigorenko, A. Nemukhin, and A. I. Krylov, "Quantum chemical benchmark studies of the electronic properties of the green fluorescent protein chromophore. 1. electronically excited and ionized states of the anionic chromophore in the gas phase," J. Chem. Theory Comput. **5**, 1895–190 (2009).
[67]P. Schellenberg, E. Johnson, A. P. Esposito, P. J. Reid, and W. W. Parson, "Resonance raman scattering by the green fluorescent protein and an analogue of its chromophore," J. Phys. Chem. B **105**, 5316–5322 (2001).
[68]T. J. Zuehlsdorff and C. M. Isborn, "Modeling absorption spectra of molecules in solution," Int. J. Quantum Chem. **119**, e25719 (2019).